

## Quark stars within relativistic models

D.P. Menezes,<sup>1,2</sup> C. Providência,<sup>3</sup> and D.B. Melrose<sup>2</sup>

<sup>1</sup> *Depto de Física - CFM - Universidade Federal de Santa Catarina  
Florianópolis - SC - CP. 476 - CEP 88.040 - 900 - Brazil*

<sup>2</sup> *School of Physics, University of Sydney, NSW 2006, Australia*

<sup>3</sup> *Centro de Física Teórica - Dep. de Física - Universidade de Coimbra - P-3004 - 516 Coimbra - Portugal*

Lately, it has been suggested that strange (quark) stars can be responsible for glitches and other observational features of pulsars. Some discussions on whether quark stars, if really exist, are bare or crusted are also a source of controversy in the recent literature. In the present work we use the Nambu-Jona-Lasinio model, known to incorporate chiral symmetry, necessarily present in the QCD formalism, in order to describe quark star properties. We compare our results for the stars and the features of the model with the much simpler model normally used in the description of strange stars, namely the MIT bag model. We also investigate the differences in the stellar properties which arise due to the presence of the crust. We show that the NJL model produces results which are somewhat different as compared with the MIT model.

PACS number(s): 26.60.+c, 24.10.Jv, 21.65.+f, 95.30.Tg

### I. INTRODUCTION AND FORMALISM

Neutron stars are the remnants of supernova explosions with masses  $1-2M_{\odot}$ , radii  $\sim 10$  km, and a temperature of the order of  $10^{11}$  K at birth, cooling within a few days to about  $10^{10}$  K by emitting neutrinos. In a conventional model for a neutron star, the star is composed of hadrons, predominantly degenerate neutrons with an admixture of protons, and degenerate electrons. In the stellar modeling, the structure of the star depends on the assumed equation of state (EOS), which contains a number of uncertainties associated with uncertainties in the strong force under conditions appropriate to a neutron star. An important uncertainty concerns the true ground state of matter. In conventional models, hadrons are assumed to be the true ground state of the strong interaction. However, it has been argued [1, 2, 3] that ‘strange matter’ is the true ground state of all matter. If this is correct, the interior of neutron stars should be composed predominantly of  $u, d, s$  quarks, plus leptons to ensure charge neutrality. This led to the suggestion that there may be no neutron stars, and that all neutron-like stars are in fact strange stars [1]. More generally, the composition of neutron stars remains a source of speculation, with some of the possibilities being the presence of hyperons [4, 5, 6], a mixed phase of hyperons and quarks [7, 8, 9, 10, 11], a phase of deconfined quarks or pion and kaon condensates [12]. Models in which the interior is assumed to be composed of strange matter are often called ‘strange’ stars. However, because, as we show, the strangeness content depends on the model used to describe the quark matter, we prefer to describe any model in which the interior involves deconvolved quarks (not bound in hyperons) as ‘quark’ stars. In the stellar modeling, the structure of the star depends on the assumed EOS, which is different in each of these cases, and which depends on the nature of the strong interaction. Apart from the differences in the EOS, an important distinction between quark stars and conventional neutron stars is that the quark stars are self-bound by the strong interaction, whereas neutron stars are bound by gravity. This allows a quark star to rotate faster than would be possible for a neutron star. Further evidence in favor of quark stars is that some stars do indeed seem to rotate faster than what would be expected for a neutron star [13, 14, 15].

A quark star must have a thin layer on its surface dominated by the electrons which are necessary to enforce charge neutrality. This layer could suspend a hadronic crust, which would not be in contact with the stellar core [1, 14]. It has been suggested that the presence of a crust provides a natural explanation for pulsar glitches [14], which are sudden changes in the rotation period of the pulsar. Other authors have argued that quark stars should be ‘bare’ [16, 17], in the sense that any such crust would either not form or would be destroyed during the supernova explosion. Recently, the characteristics of the radiation from hot, bare strange stars have been identified [18].

Possible candidates for quark stars include compact star with gravitational masses around  $\leq 1M_{\odot}$  and radii of the order of  $\simeq 6$  km: PSR J1645-0317 (PSR B1642-03), PSR J1830-1059 (PSR B1828-11) [19], RX J185635-3754 [20], Her X-1 [21], 4U 1728-34 [22], X-ray bursters GRO J1744-28 [23] and SAX J1808.4-3658 [24].

There are several different models that describe quark matter. In [25] we investigated the properties of strange stars using two different models: the MIT bag model [26], which is widely favored in the literature on strange stars, and the color-favor-locked phase (CFL) model [27], which allows the quarks near the Fermi surface to form Cooper pairs which condense and break the color gauge symmetry [28]. At sufficiently high density the favored phase is called CFL, in which quarks of all three colors and all three flavors are allowed to pair. In [25] we verified that quark stars have different maximum gravitational and baryonic masses, compared with neutron stars, and that the maximum masses are not significantly affected by the presence or absence of a crust. Moreover, with a simple prescription for the Kepler frequency, which determines the spin rate of a neutron-like star, we obtained much higher values for the quark stars than for the neutron stars. Finally, in [25] we used the two possible mass-to-radius ratio constraints available in the literature [29, 30] to distinguish between the assumed EOSs. Concerning one of the constraints, specifically the interpretation of absorption features as atomic transition lines in [30] is controversial: an alternative interpretation [31, 32] is that the absorption features are cyclotron lines, which imply no obvious constraint on the EOS. However, if the accepted interpretation is correct, then only the quark star EOS is compatible with the constraint given in [29], thereby excluding most of the neutron star EOSs. The conclusion that all neutron stars must be quark stars has major implications, but it is necessarily valid only for either of the two EOSs investigated in [25].

In the present paper we focus on a different model for the strange matter, the Nambu-Jona-Lasinio (NJL) model [33]. Our aim is to use this model to obtain the stellar properties and compare the results with the MIT bag model [26]. It is important to distinguish between the EOS during the short time period when neutrinos are still trapped in the star, and the EOS after the neutrinos escape. The maximum entropy per baryon ( $S$ ) reached in the core of a new born star is about 2 (in units of Boltzmann's constant) [34]. We then perform our calculations for  $S = 0$  ( $T = 0$ ), 1 and 2 since the entropy and not the temperature should be constant throughout the star [35].

In section II the formalism used is presented; in section III we give the results and make the relevant discussions and in section IV the conclusions are drawn.

## II. QUARK MATTER MODELS

In this section we summarize the main formulae for both models used in this paper.

### A. The Nambu-Jona-Lasinio Model

We choose the NJL model [36, 37, 38, 39] to describe the quark phase. The SU(3) version of the model includes most of symmetries of QCD, including chiral symmetry, and its breaking, which is essential in treating the lightest hadrons. The NJL model also includes a scalar-pseudoscalar interaction and the 't Hooft six fermion interaction that models the axial  $U(1)_A$  symmetry breaking. The NJL model assumes deconfined point-like quarks, and is not renormalizable, requiring regularization through a cutoff in three-momentum space.

The NJL model is defined by the Lagrangian density

$$L = \bar{q}(i\gamma^\mu\partial_\mu - m)q + g_S \sum_{a=0}^8 [(\bar{q}\lambda^a q)^2 + (\bar{q}i\gamma_5\lambda^a q)^2] + g_D \{ \det [\bar{q}_i(1 + \gamma_5)q_j] + \det [\bar{q}_i(1 - \gamma_5)q_j] \}, \quad (1)$$

where  $q = (u, d, s)$  are the quark fields and  $\lambda_a$  ( $0 \leq a \leq 8$ ) are the U(3) flavor matrices. The model parameters are:  $m = \text{diag}(m_u, m_d, m_s)$ , the current quark mass matrix ( $m_d = m_u$ ), the coupling constants  $g_S$  and  $g_D$  and the cutoff in three-momentum space,  $\Lambda$ . The NJL model is valid only for quark momenta smaller than the cut-off  $\Lambda$ .

The set of parameters is chosen in order to fit the values in vacuum for the pion mass, the pion decay constant, the kaon mass and the quark condensates. We consider the set of parameters [39, 40]:  $\Lambda = 631.4 \text{ MeV}$ ,  $g_S \Lambda^2 = 1.824$ ,  $g_D \Lambda^5 = -9.4$ ,  $m_u = m_d = 5.6 \text{ MeV}$  and  $m_s = 135.6 \text{ MeV}$  which are fitted to the following properties:  $m_\pi = 139 \text{ MeV}$ ,  $f_\pi = 93.0 \text{ MeV}$ ,  $m_K = 495.7 \text{ MeV}$ ,  $f_K = 98.9 \text{ MeV}$ ,  $\langle \bar{u}u \rangle = \langle \bar{d}d \rangle = -(246.7 \text{ MeV})^3$  and  $\langle \bar{s}s \rangle = -(266.9 \text{ MeV})^3$ .

The thermodynamical potential density is given by  $\Omega = \mathcal{E} - TS - \sum_i \mu_i N_i - \Omega_0$ , where the energy

density is

$$\begin{aligned} \mathcal{E} = & -2 N_c \sum_i \int \frac{d^3 p}{(2\pi)^3} \frac{p^2 + m_i M_i}{E_i} (n_{i-} - n_{i+}) \theta(\Lambda^2 - p^2) \\ & - 2 g_S \sum_{i=u,d,s} \langle \bar{q}_i q_i \rangle^2 - 2 g_D \langle \bar{u} u \rangle \langle \bar{d} d \rangle \langle \bar{s} s \rangle - \mathcal{E}_0 \end{aligned} \quad (2)$$

and the entropy density is

$$S = -2 N_c \sum_{i=u,d,s} \int \frac{d^3 p}{(2\pi)^3} \theta(\Lambda^2 - p^2) \{ [n_{i+} \ln(n_{i+}) + (1 - n_{i+}) \ln(1 - n_{i+})] + [n_{i+} \rightarrow n_{i-}] \}. \quad (3)$$

In the above expressions  $N_c = 3$ ,  $T$  is the temperature,  $\mu_i$  ( $N_i$ ) is the chemical potential (number) of particles of type  $i$ , and  $\mathcal{E}_0$  and  $\Omega_0$  are included in order to ensure  $\mathcal{E} = \Omega = 0$  in the vacuum. This requirement fixes the density independent part of the EOS. The ground state of the system is described by the density matrix [39] given by  $f = \text{diag}(f_u, f_d, f_s)$  with

$$f_i = \frac{1}{2} [I (n_{i-} + n_{i+}) - \frac{\gamma^0 M_i + \boldsymbol{\alpha} \cdot \mathbf{p}}{E_i} (n_{i-} - n_{i+})] \theta(\Lambda^2 - p^2), \quad (4)$$

where  $I$  is the identity matrix,  $n_i^{(\mp)}$  are the Fermi distribution functions of the negative (positive) energy states,  $n_i^{(\mp)} = [1 + \exp(\mp(\beta(E_i \pm \mu_i)))]^{-1}$ ,  $i = u, d, s$ . In the last equation  $\beta = 1/T$ ,  $M_i$  is the constituent quark mass,  $E_i = (p^2 + M_i^2)^{1/2}$ .

The quark condensates and the quark densities are defined, for each of the flavors  $i = u, d, s$ , respectively, as:

$$\langle \bar{q}_i q_i \rangle = -2 N_c \int \frac{d^3 p}{(2\pi)^3} \frac{M_i}{E_i} (n_{i-} - n_{i+}) \theta(\Lambda^2 - p^2), \quad (5)$$

$$\rho_i = \langle q_i^\dagger q_i \rangle = 2 N_c \int \frac{d^3 p}{(2\pi)^3} (n_{i-} + n_{i+} - 1) \theta(\Lambda^2 - p^2). \quad (6)$$

Minimizing the thermodynamical potential  $\Omega$  with respect to the constituent quark masses  $M_i$  leads to three gap equations for the masses  $M_i$

$$M_i = m_i - 4 g_S \langle \bar{q}_i q_i \rangle - 2 g_D \langle \bar{q}_j q_j \rangle \langle \bar{q}_k q_k \rangle, \quad (7)$$

with cyclic permutations of  $i, j, k$ .

We introduce an effective dynamical Bag pressure [41],

$$\begin{aligned} B = & 2 N_c \sum_{i=u,d,s} \int \frac{d^3 p}{(2\pi)^3} \left( \sqrt{p^2 + M_i} - \sqrt{p^2 + m_i} \right) \theta(\Lambda^2 - p^2) \\ & - 2 g_S \sum_{i=u,d,s} \langle \bar{q}_i q_i \rangle^2 - 4 g_D \langle \bar{u} u \rangle \langle \bar{d} d \rangle \langle \bar{s} s \rangle. \end{aligned}$$

In terms of this quantity the energy density (2) takes the form

$$\mathcal{E} = 2 N_c \sum_{i=u,d,s} \int \frac{d^3 p}{(2\pi)^3} \sqrt{p^2 + M_i} (n_{i+} - n_{i-} + 1) \theta(\Lambda^2 - p^2) + B_{eff}, \quad B_{eff} = B_0 - B, \quad (8)$$

where  $B_0 = B_{\rho_u = \rho_d = \rho_s = 0}$ . Writing the energy density in terms of  $B_{eff}$  allows us to identify this contribution as a Bag pressure and establish a relation with the MIT Bag model [33, 41] discussed in the next section.

## B. The MIT Bag Model

The MIT Bag model [26] has been extensively used to describe quark matter. In its simplest form, the quarks are considered to be free inside a Bag and the thermodynamic properties are derived from the Fermi gas model. The energy density, the pressure and the quark  $q$  density, respectively, are given by

$$\mathcal{E} = 3 \times 2 \sum_{q=u,d,s} \int \frac{d^3p}{(2\pi)^3} \sqrt{\mathbf{p}^2 + m_q^2} (f_{q+} + f_{q-}) + Bag, \quad (9)$$

$$P = \frac{1}{\pi^2} \sum_q \int dp \frac{\mathbf{p}^4}{\sqrt{\mathbf{p}^2 + m_q^2}} (f_{q+} + f_{q-}) - Bag, \quad (10)$$

$$\rho_q = 3 \times 2 \int \frac{d^3p}{(2\pi)^3} (f_{q+} - f_{q-}), \quad (11)$$

where 3 stands for the number of colors, 2 for the spin degeneracy,  $m_q$  for the quark masses,  $Bag$  represents the bag pressure and the distribution functions for the quarks and anti-quarks are the Fermi distributions

$$f_{q\pm} = 1/(1 + \exp[(\epsilon \mp \mu_q)/T]), \quad (12)$$

with  $\mu_q$  ( $-\mu_q$ ) being the chemical potential for quarks (anti-quarks) of type  $q$  and  $\epsilon = (\mathbf{p}^2 + m_q^2)^{1/2}$ . These equations apply at nonzero temperatures. For  $T = 0$ , there are no antiparticles, and the particle distribution functions become the usual step functions.

We use  $m_u = m_d = 5.5$  MeV,  $m_s = 150.0$  MeV and  $Bag = (180 \text{ MeV})^4$ . If  $m_u$ ,  $m_d$  and  $m_s$  are chosen as in the NJL model, the behavior of the properties of interest are not altered, since they are more dependent on the Bag pressure than on small differences in the quark masses.

## C. Quark matter in beta equilibrium

In a star with quark matter we must impose both beta equilibrium and charge neutrality [15]. In what follows two scenarios are investigated, an early stage when there are trapped neutrinos in the interior of the star and a later stage, after the neutrinos escape (deleptonization). We first consider the later stage when entropy is maximum and neutrinos diffuse out. The neutrino chemical potential is then zero. For  $\beta$ -equilibrium matter we must add the contribution of the leptons as free Fermi gases (electrons and muons) to the energy and pressure. The relations between the chemical potentials of the different particles are given by

$$\mu_s = \mu_d = \mu_u + \mu_e, \quad \mu_e = \mu_\mu. \quad (13)$$

For charge neutrality we must impose

$$\rho_e + \rho_\mu = \frac{1}{3}(2\rho_u - \rho_d - \rho_s).$$

For the electron and muon densities we have

$$\rho_l = 2 \int \frac{d^3p}{(2\pi)^3} (f_{l+} - f_{l-}), \quad l = e, \mu, \quad (14)$$

where the distribution functions for the leptons are given in eq. (12) by substituting  $q$  by  $l$ , with  $\mu_l$  the chemical potential for leptons of type  $l$ . At  $T = 0$ , eq. (14) becomes  $\rho_l = k_{Fl}^3/3\pi^2$ . The pressure for the leptons is

$$P_l = \frac{1}{3\pi^2} \sum_l \int \frac{\mathbf{p}^4 dp}{\sqrt{\mathbf{p}^2 + m_l^2}} (f_{l+} + f_{l-}). \quad (15)$$

In earlier stage, when the neutrinos are still trapped in the interior of the star, eq. (13) is replaced by

$$\mu_s = \mu_d = \mu_u + \mu_e - \mu_{\nu e}, \quad (16)$$

the lepton contribution is set to be  $Y_L = Y_e + Y_{\nu e} = 0.4$  [35]. No muons appear in this case.

### III. RESULTS

In order to describe the crust of the quark stars we next use the well known EOS calculated in [42] for very low densities.

In figure 1 the strange quark mass as a function of the density is shown for the NJL models and the 6 cases discussed in the present work, i.e.,  $S = 0, 1, 2$  without neutrinos and with trapped neutrinos. These data have a substantial influence on the results we obtain with the NJL model. Chiral symmetry restoration occurs first for the  $u$  and  $d$  quarks and only at higher densities for the  $s$  quarks. This is clearly seen in figure 1: the mass of the  $s$ -quark starts to decrease only for  $\rho/\rho_0 > 4$  (6) for neutrino free (trapped) matter.

In figure 2 we show the EOS obtained respectively for the MIT bag and for the NJL models again for the 6 different cases mentioned above. As shown in the upper panel in figure 2, the results are very similar and it is difficult to distinguish between them; this may be attributed to the familiar result that for an extreme relativistic gas the pressure is one third of the energy density. The NJL model presents different behaviors at high densities. The fact that chiral symmetry is restored at different densities for quarks with different masses explains the softer behavior of the EOS for  $\epsilon > 4 \text{ fm}^{-4}$ . At these densities the onset of strangeness occurs, with the onset occurring at larger densities when neutrino trapping is included (see Fig. 1). The EOS with trapped neutrinos is harder and the  $S = 0, 1, 2$  cases are similar, but distinguishable since higher temperatures correspond to harder EOSs. This behavior was already seen in [11], although in a different context.

In figure 3 we show the temperature range described by both models for the cases  $S = 1$  and  $S = 2$ . For the MIT model, the temperature for each different EOS increases steadily, reaching about 35 MeV for  $S = 2$  and  $\simeq 17$  MeV for  $S = 1$  at  $\rho = 12\rho_0$ . The NJL model presents a different behavior: the temperature first oscillates before increasing. The near-plateau around 4–6  $\rho/\rho_0$  coincides with the onset of strangeness opening of a new degree of freedom. The maximum temperature for  $S = 2$  without neutrinos is higher than the one obtained with the MIT model for the same energy density. This difference is due to the fact that within the MIT model the fractions of the different types of quarks are similar, unlike the NJL which has a smaller fraction of  $s$ -quarks, which gives rise to a higher entropy. If we fix the entropy the temperature must be lower within the MIT model. However, from Table I we can see that within the NJL the central energy densities of compact stars are much lower than the corresponding ones for the MIT model. The temperatures are not shown in Table I because they vary though the star; the temperatures in the interior of the quark stars are then similar for the NJL and the MIT models, despite the significant difference in density. Including trapped neutrinos lowers the temperature of the star. This is due to the presence of a fixed fraction of leptons increasing the degrees of freedom, and then to keep the entropy per particle and the thermodynamic potential fixed, a lower temperature is required. If neutrino trapping is not imposed the fraction of leptons in the star is very small.

In figure 4 we plot the strangeness content in each situation described in the text. As already referred, within the NJL the onset of strangeness occurs for  $\rho/\rho_0 \sim 4$  depending on the temperature and the neutrino content. A different situation applies for the MIT bag: strangeness is present from lower densities and at  $\rho/\rho_0 \sim 4$  the strangeness fraction is almost at its maximum value in the case without neutrinos,  $\sim 0.33$ . The presence of leptons in the case of trapped neutrinos with a fixed lepton fraction lowers the strangeness content due to the electric charge conservation restrictions.

In figure 5 we display, for both the MIT and the NJL models, the electron neutrino fraction present in the interior of the stars when trapped neutrinos are included. With the MIT model the neutrino content is practically the same for the three entropies considered. It increases a little for lower densities and then reaches its maximum value, for the same reasons discussed above, i.e., neutrinos and electrons together are fixed to a certain fraction and electrons compensate for charge neutrality in a system where the three quarks have equal number densities. The NJL model shows a slight decrease in the neutrino fraction until the onset of strangeness. This effect is more pronounced for  $\rho < 3\rho_0$  when chiral symmetry restoration has still not occurred for the  $u$  and  $d$  quarks. A slight increase in the neutrino fraction occurs with the increase of the entropy, mainly at low densities. The neutrino fraction never reaches 14% within the NJL picture, but it amounts to more than 15% within the MIT model. We see a similar neutrino fraction for these models in [10, 11]. The difference in neutrino content is again due to the larger fraction of strange quarks in the MIT description and therefore a smaller number density of electrons required by the electric charge neutrality. A smaller fraction of electrons implies a larger fraction of neutrinos for a fixed lepton fraction. Nevertheless, if the CFL model were used for the quark matter with trapping, a much higher neutrino fraction, of the order of 35%, would be possible [10].

Given the EOS, the next step is to solve the Tolman-Oppenheimer-Volkoff equations [43]. Table I lists the main properties of the stars, including their maximum gravitational and baryonic masses, their radii and central energy densities, for all the EOSs considered in the present work. As expected, quark stars

have smaller maximum masses with smaller radii [9, 10, 25] and higher central densities.

Let us first analyze the results obtained with the MIT model and then outline the main differences that appear with the NJL model. For quark stars either without or with neutrinos, the maximum gravitational masses and radii are always around  $1.23\text{--}1.24 M_\odot$  and  $6.7\text{--}7.1$ , respectively, and the energy density is around  $14.5 \text{ fm}^{-4}$ . The inclusion of trapped neutrinos and a crust, have practically no effect on the numerical results.

The NJL model leads to significantly different results. The maximum masses and radii are systematically larger and, as a consequence, the central energy densities are lower than for the MIT bag model. In fact, the results do not depend strongly on the entropy, as already pointed out in [25]. In the NJL, for a bare star without neutrinos, the maximum masses and radii decrease and the central energy density increases as the entropy increases. For a star with a crust, the gravitational and baryonic masses decrease but the radii oscillate as the entropy increases.

In Fig. 6 we show for  $S = 0$ , and for both models the mass-radius plot of the family of stars obtained for the neutrino free and the neutrino trapped situations. It is clear that the NJL predicts the possibility of existence of more massive and with larger radius stars. For a fixed radius smaller than the larger accepted by the MIT model the NJL gives stars with much smaller gravitation masses. Conclusions for finite entropies are the same.

Another difference is that when trapped neutrinos are included, this generally increases the maximum gravitational mass, with the increase being much larger for the NJL than for the MIT model.

In a previous work [25] we see that the MIT results are sensitive to the *Bag* parameter. With a lower value of this parameter, results similar to the ones obtained with the NJL model are found. The same is possible when the CFL model is used. In [25] we fixed the gap parameter of the CFL model as  $100 \text{ MeV}$  and showed that the properties of the star depend on the *Bag* parameter, but the properties are also known to depend on the gap parameter [44].

It is not clear that quark stars really exist, and if they do exist in principle, how they would be formed. They form directly in a supernova explosion, or as a consequence of the hadron-quark deconfinement phase transition in stellar compact stars [45]. In the former case there is neutrino trapping during the first seconds of the stars life and the entropy is approximately constant throughout the star [35]. In this case one concludes from our results that there can be no late blackhole formation. This event is only possible if the baryonic mass of a stable star at finite temperature is larger than the largest baryonic mass of a stable cold star [34]. From Table I one can see that the maximum baryonic masses at fixed entropies are always lower than the corresponding values at zero temperature. This kind of effect could occur within hybrid stars [11, 34].

From figure 6 and Table I we can also see that the inclusion of a crust has a similar effect for both the MIT and NJL models: the radius of the maximum mass star increases  $\sim 0.3 \text{ km}$ . It has been argued that at finite temperature the star tends to be bare due to the reduction of the electrostatic potential of the electron [46]. In particular, at  $T = 30 \text{ MeV}$  a star has essentially no crust. Taking into account simulations with neutron stars, we should consider the entropy rather than the temperature to be constant throughout the star [35]. In this case the temperature at the surface is lower: we get  $\sim 8$  and  $16 \text{ MeV}$  respectively for  $S = 1$  and  $S = 2$ , respectively.

An important difference between the NJL stars and MIT stars is that the electron chemical potential is very different. In Fig. 7a we show, as a function of the density, the electron chemical potential in both models for the different values of entropy. Entropy has almost no effect on the results but there is an important difference between the MIT and the NJL cases:  $\mu_e < 20 \text{ MeV}$  for the MIT model and  $\mu_e$  as high as  $100 \text{ MeV}$  for the NJL model. In the interior of a star the electron chemical potential is shown to be equal to the electric potential energy [46, 47]. In figure 7b we plot this quantity for stars with  $M = 1.2 M_\odot$  for NJL (thick lines) and MIT (thin lines), and for stars with  $M = 1.4 M_\odot$  for NJL (thick lines). In the last two cases, which correspond to stars close to the maximum mass for a stable star, the curves for  $S = 0, 1$  and  $2$  are almost coincident and so we have only plotted the  $S = 0$  curve.

One of the motivations of this work was to verify whether, with the NJL model, the presence or absence of a crust on a quark star affects its properties and how these properties differ from those obtained with the MIT model. We already knew that within the MIT and the CFL models the differences are non-negligible [25]. From Table I and Fig. 6 the presence of the crust, described by the BPS EOS [42], affects the MIT model than the NJL model. With the NJL model the main differences appear in the radius and the central energy density.

We note that our results are different from those obtained in [48], where a lower maximum mass was obtained, probably due to a different choice of the parametrization for the NJL model.

TABLE I: Quark star properties for the EOSs described in the text.

type	crust	entropy	neutrinos	$M_{\max}$	$M_{b\max}$	$R$	$\varepsilon_0$
				( $M_{\odot}$ )	( $M_{\odot}$ )	(km)	( $\text{fm}^{-4}$ )
MIT	no	0	no	1.22	1.29	6.77	14.53
MIT	no	1	no	1.23	1.28	6.78	14.35
MIT	no	2	no	1.23	1.26	6.77	14.73
MIT	yes	0	no	1.23	1.21	7.10	14.61
MIT	yes	1	no	1.23	1.20	7.06	14.67
MIT	yes	2	no	1.23	1.18	7.01	14.54
MIT	no	0	yes	1.24	1.19	6.82	14.36
MIT	no	1	yes	1.23	1.18	6.81	14.52
MIT	no	2	yes	1.24	1.18	6.86	13.98
MIT	yes	0	yes	1.24	1.03	7.10	14.41
MIT	yes	1	yes	1.24	1.02	7.11	14.41
MIT	yes	2	yes	1.24	1.00	7.11	14.41
NJL	no	0	no	1.47	1.56	9.03	7.26
NJL	no	1	no	1.47	1.54	9.02	7.46
NJL	no	2	no	1.46	1.51	9.01	7.60
NJL	yes	0	no	1.47	1.55	9.34	7.44
NJL	yes	1	no	1.47	1.53	9.35	7.52
NJL	yes	2	no	1.46	1.50	9.29	7.76
NJL	no	0	yes	1.56	1.57	8.99	8.07
NJL	no	1	yes	1.55	1.55	8.99	8.04
NJL	no	2	yes	1.54	1.53	9.00	8.07
NJL	yes	0	yes	1.56	1.56	9.26	8.15
NJL	yes	1	yes	1.55	1.55	9.23	8.19
NJL	yes	2	yes	1.54	1.52	9.25	8.23

#### IV. CONCLUSIONS

In this paper we consider the properties of quark stars with the NJL model for the EOS. This model has more realistic features than the MIT bag model, in particular, chiral symmetry. Due to the large  $s$ -quark mass at low densities, several features of the NJL stars are different from the corresponding quantities for the MIT stars: smaller strangeness content, higher electron chemical potentials, smaller neutrino fractions in stars with trapped neutrinos, higher maximum star masses and smaller maximum central densities. In fact, the properties of quark stars with the NJL model are closer to the corresponding properties of hybrid stars, e.g. maximum masses, than to the properties of the MIT quark stars.

We also show that if a quark star is formed directly from a supernova explosion there can be no delayed blackhole formation, because the maximum baryonic masses of hot stars are always smaller than the corresponding masses of cold stars.

The electron chemical potential inside the stars has quite large values with the NJL model. This influences the properties of the surface of a quark star and the possibility of crust formation.

#### Acknowledgements

This work was partially supported by Capes (Brazil) under process BEX 1681/04-4, CAPES (Brazil)/GRICES (Portugal) under project 100/03 and FEDER/FCT (Portugal) under the project POCTI/FP/FNU/50326/2003. D.P.M. would like to thank the friendly atmosphere at the Reserch Centre

for Theoretical Astrophysics, Sydney University, where this work was done.

- 
- [1] C. Alcock, E. Farhi and A. Olinto, *Astrophys. J.* **310**, 261 (1986).
- [2] A.R. Bodmer, *Phys. Rev.* **D 4**, 1601 (1971).
- [3] E. Witten, *Phys. Rev.* **D 30**, 272 (1984).
- [4] A. L. Espíndola and D. P. Menezes, *Phys. Rev.* **C 65**, 045803 (2002).
- [5] A.M.S. Santos and D.P. Menezes, *Phys. Rev.* **C 69**, 045803 (2004).
- [6] R. Cavagnoli and D.P. Menezes, *Braz. J. Phys.* (2005), in press; nucl-th/0506064.
- [7] D.P. Menezes and C. Providência, *Phys. Rev.* **C 68**, 035804 (2003).
- [8] D.P. Menezes and C. Providência, *Phys. Rev.* **C 70**, 058801 (2004); D.P. Menezes and C. Providência, *Braz. J. Phys.* **34**,724 (2004).
- [9] P.K. Panda, D.P. Menezes and C. Providência, *Phys. Rev.* **C 69**, 025207 (2004).
- [10] P.K. Panda, D.P. Menezes and C. Providência, *Phys. Rev.* **C 69**, 058801 (2004).
- [11] D.P. Menezes and C. Providência, *Phys. Rev.* **C 69**, 045801 (2004).
- [12] D.P. Menezes, P.K. Panda and C. Providência, *Phys. Rev.* **C** (2005), in press; astro-ph/0506196.
- [13] J.A. Frieman and A.V. Olinto, *Nature* **341**, 633 (1989).
- [14] N. K. Glendenning and F. Weber, *Astrophys. J.* **400**, 647 (1992).
- [15] N. K. Glendenning, *Compact Stars*, Springer-Verlag, New-York, 2000.
- [16] R.X. Xu, *Strange Quark Stars - A Review*, in: *High Energy Processes, Phenomena in Astrophysics*, Proceedings of IAU Symposium No. 214, eds. X. D.Li, Z. R. Wang and V. Trimble, p.191-198
- [17] V.V. Usov, *Phys. Rev. Lett.* **80**, 230 (1998); *Astrophys. J.* **550**, L179 (2001a).
- [18] A.G. Aksenov, M. Milgrom and V.V. Usov, *Astrophys. J.* **609**, 363 (2004).
- [19] J.H. Taylor, R.N. Manchester and A.G. Lyne, *The Astrophys. J. Suppl. Series* 88, 529 (1993).
- [20] J. Pons, F.M. Walter, J.M. Lattimer et.al., *Astrophys. J.* **564**, 981 (2002).
- [21] X.D. Li, Z.G. Lai and Z.R. Wang, *Astron. and Astrophys.* **303** L1 (1995).
- [22] X.D. Li, S. Ray, J. Dey, M. Dey and I. Bombaci, *Astrophys. J.* **527**, L51 (1999b).
- [23] K.S. Cheng, Z.G. Dai, D.M. Wai and T. Lu, *Science* **280**, 407 (1998).
- [24] X. Li, I. Bombaci, M. Dey, J. Dey and E.P.J. van den Heuvel, *Phys. Rev. Lett.* **83**, 3776 (1999a).
- [25] D.P. Menezes and D.B. Melrose, astro-ph/0506158, submitted to *Publ. Astr.Soc. Aust.*
- [26] A. Chodos, R.L. Jaffe, K. Johnson, C.B. Thorne and V.F. Weisskopf, *Phys. Rev.* **D 9**, 3471 (1974).
- [27] I. Shovkovy, M. Hanauske, M. Huang, *Phys. Rev. D* **67**, 103004 (2003); D. T. Son and M. Stephanov, *Phys. Rev D* **61**, 074012 (2000); **62**, 059902(E) (2000); M. Alford and S. Reddy, *Phys. Rev. D* **64**, 074024 (2003).
- [28] M.G. Alford, *Annu. Rev. Nucl. Part. Sci.* **51** 131 (2001).
- [29] J. Cottam, F. Paerels and M. Mendez, *Nature* **420**, 51 (2002).
- [30] D. Sanwal, G.G. Pavlov, V.E. Zavlin and M.A. Teter, *Astrophys. J.* **574**, L 61 (2002).
- [31] G.F. Bignami, P.A. Caraveo, A. De Luca and S. Mereghetti, *Nature* **423**, 725 (2003).
- [32] R.X. Xu, H.G. Wang and G.J. Qiao, *Chin. Phys. Lett.* **20**, 314 (2003).
- [33] Y. Nambu and G. Jona-Lasinio, *Phys. Rev.* **122**, 345 (1961); **124**, 246 (1961).
- [34] M. Prakash, I. Bombaci, M. Prakash, P. J. Ellis, J. M. Lattimer and R. Knorren, *Phys. Rep.* **280**, 1 (1997).
- [35] A. Burrows and J. M. Lattimer, *Astrophys. J.* **307**, 178 (1986).
- [36] S. P. Klevansky, *Rev. Mod. Phys.* **64** (1992) 649; P. Zuang, J. Hüfner and S. P. Klevansky, *Nucl. Phys. A* **576** (1994) 525.
- [37] T.Hatsuda and T. Kunihiro, *Phys. Rep.* **247** (1994) 221.
- [38] J. da Providência, M. C. Ruivo and C. A. de Sousa, *Phys. Rev. D* **36** (1987) 1882; M. C. Ruivo, C. A. de Sousa, B. Hiller and A. H. Blin, *Nucl. Phys. A* **575** (1994) 460.
- [39] C. Ruivo, C. Sousa and C. Providência, *Nucl. Phys. A* **651** (1999) 59.
- [40] T. Kunihiro, *Phys. Lett.* **B 219**, 363 (1989).
- [41] M. Buballa and M. Oertel, *Phys. Lett.* **B 457**, 261 (1999); K. Schertler, S. Leupold and J. Schaffner-Bielich, *Phys. Rev C* **60**, 025801 (1999).
- [42] G.Baym, C. Pethick and P. Sutherland, *Astrophys. J.* **170**, 299 (1971).
- [43] R.C. Tolman, *Phys. Rev.* **55** (1939) 364; J.R. Oppenheimer and G.M. Volkoff, *Phys. Rev.* **55** (1939) 374.
- [44] G. Lugones and J.E. Horvath, *Phys. Rev. D* **66**, 074017 (2002); *Astron. and Astrophys.* **403**, 173 (2003).
- [45] I. Bombaci, I. Parenti and I. Vidaña, *Astrophys. J.* **614**, 314 (2004).
- [46] Ch. Kettner, F. Weber, M. K. Weigel and N. K. Glendenning, *Phys. Rev. D* **51**, 1440 (1995).
- [47] T. Chmaj and W. Slominski, *Phys. Rev. D* **40**, 165 (1989).
- [48] M. Hanauske, L.M. Satarov, I.N. Mishustin, H. Stocker and W. Greiner, *Phys. Rev. D* **64**, 043005 (2001).



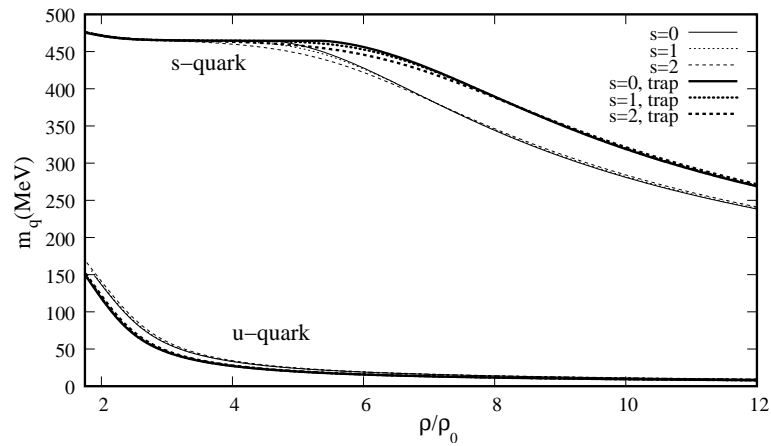


FIG. 1: the  $u$  and  $s$ -quark mass as a function of density within the NJL for the different entropies with (thick lines) and without (thin lines) neutrino trapping

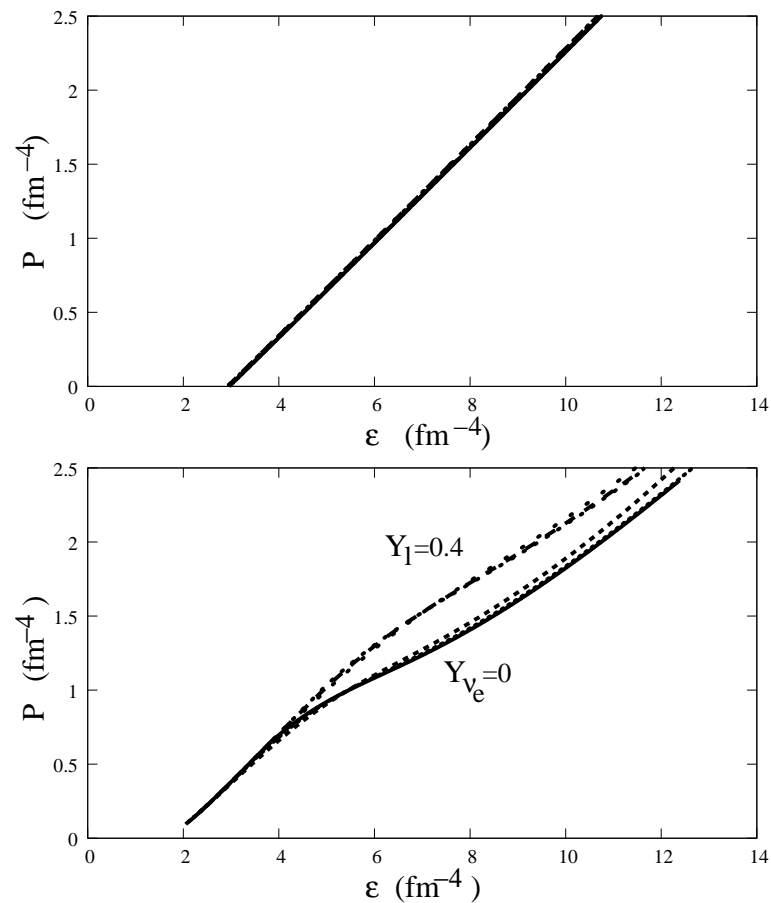


FIG. 2: EOS obtained for  $S = 0, 1, 2$  without neutrinos and with trapped neutrinos within the MIT bag model (top figure) and the NJL model (bottom figure).  $S = 0$  gives always the softer and  $S = 2$  the harder EOS.

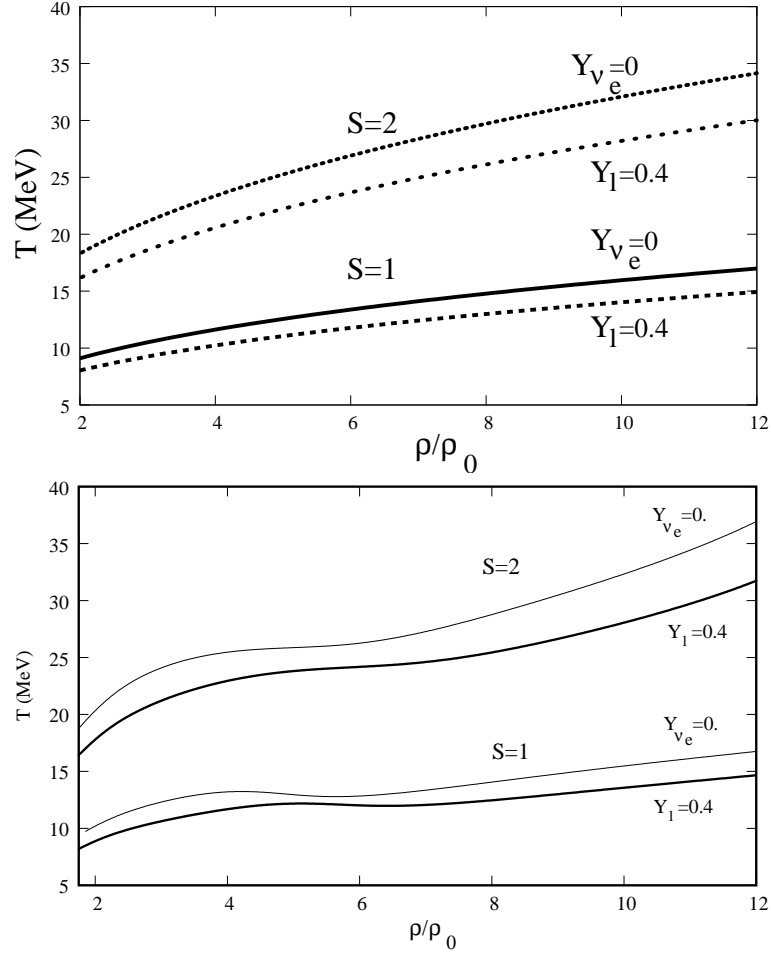


FIG. 3: Temperature range obtained for  $S = 1, 2$  without neutrinos and with trapped neutrinos within the MIT bag model (top figure) and the NJL model (bottom figure).

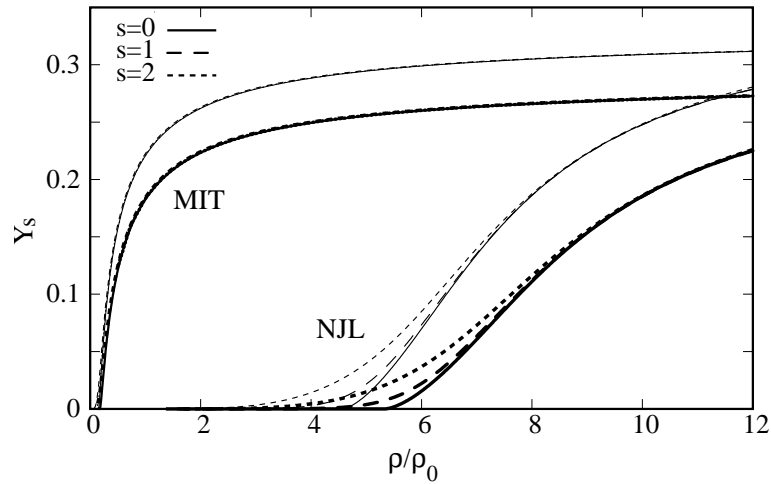


FIG. 4: Strangeness content obtained for  $S = 0, 1, 2$  without neutrinos and with trapped neutrinos within the MIT bag model (top figure) and the NJL model (bottom figure).

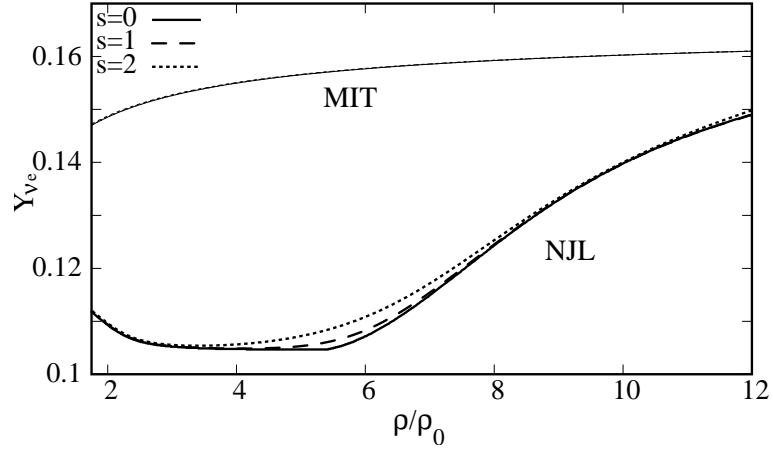


FIG. 5: Neutrino fraction obtained for  $S = 0, 1, 2$  within the MIT bag model (top curves) and the NJL model (bottom curves).

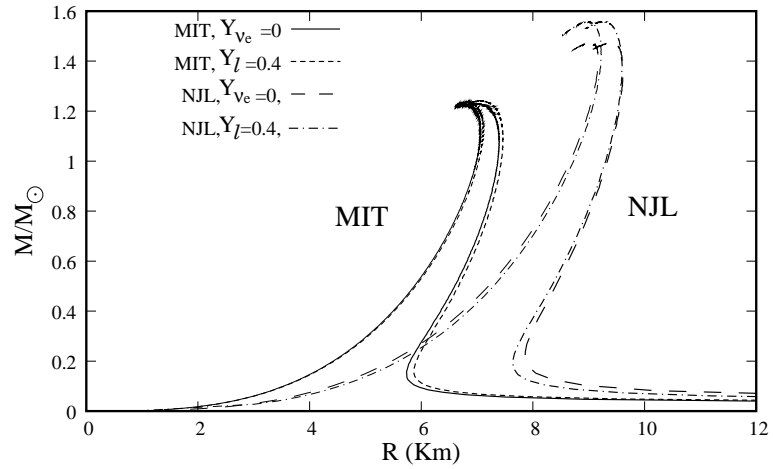


FIG. 6: Mass-radius plots for bare and crusted MIT and NJL stars at  $S = 0$  with and without neutrinos.

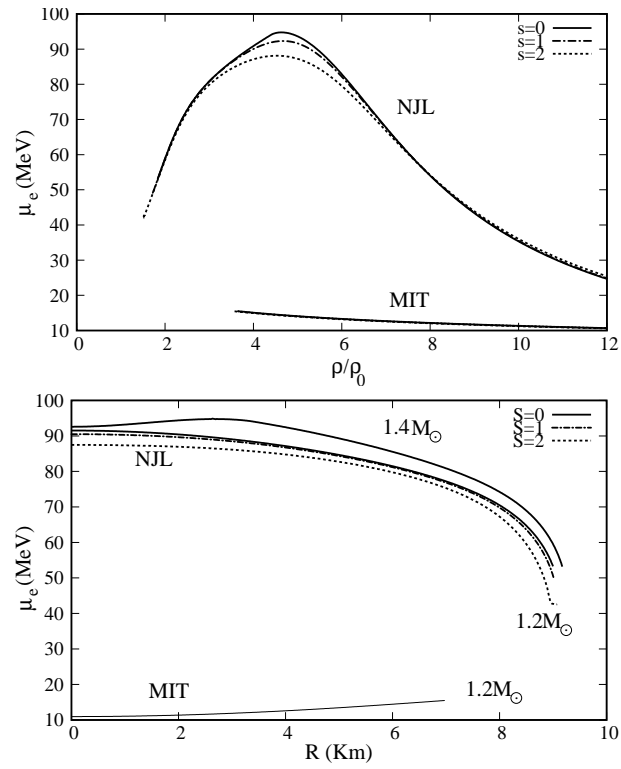


FIG. 7: The electron chemical potential a) as a function of density; b) in the interior of stars with  $M = 1.2$  and  $1.4 M_\odot$ . Thin lines are for the MIT model and thick lines for the NJL.